Acta Crystallographica Section F
Structural Biology and Crystallization Communications
ISSN 1744-3091

Crystallization and preliminary X-ray crystallographic analysis of the [NiFe]-hydrogenase maturation factor HypF1 from *Ralstonia eutropha* H16

Gordon Winter,[a,b] Simon Dökel,[a,b] Anne K. Jones,[a]‡ Patrick Scheerer,[b]§ Norbert Krauss,[b]*¶ Wolfgang Höhne[b] and Bärbel Friedrich[a]

[a]Institut für Biologie/Mikrobiologie, Humboldt-Universität zu Berlin, Chausseestrasse 117, D-10115 Berlin, Germany, and [b]Institut für Biochemie, Charité-Universitätsmedizin Berlin, Monbijoustrasse 2a, D-10117 Berlin, Germany

‡ Present address: Department of Chemistry and Biochemistry, Arizona State University, Tempe, Arizona 85287, USA.
§ Present address: Institut für Medizinische Physik und Biophysik, Charité-Universitätsmedizin Berlin, Ziegelstrasse 5-9, D-10098 Berlin, Germany.
¶ Present address: Queen Mary University of London, School of Biological and Chemical Sciences, Mile End Road, London E1 4NS, England.

Correspondence e-mail: n.krauss@qmul.ac.uk

Received 15 December 2009
Accepted 16 February 2010

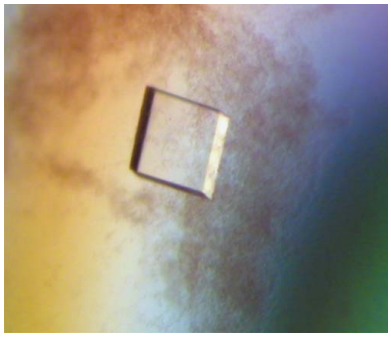

The hydrogenase maturation factor HypF1 is a truncated but functional version of the HypF protein. HypF is known to be involved in the supply of the CN^- ligands of the active site of [NiFe]-hydrogenases, utilizing carbamoyl phosphate as a substrate. The first crystallization and preliminary X-ray studies of HypF1 from *Ralstonia eutropha* H16 are reported here. Crystals of HypF1 (394 amino acids, 40.7 kDa) were obtained by the sitting-drop vapour-diffusion technique using sodium formate as a precipitant. The crystals belonged to space group *I*222, with unit-cell parameters $a = 79.7$, $b = 91.6$, $c = 107.2$ Å. Complete X-ray diffraction data sets were collected at 100 K from native crystals and from a platinum derivative to a maximum resolution of 1.65 Å.

1. Introduction

Hydrogenases are widespread among all domains of microorganisms and catalyze the oxidation of hydrogen and the reverse reaction, the reduction of protons to molecular hydrogen. Their catalysis of this biotechnologically important process has brought them into the spotlight as potential catalysts for the production or utilization of hydrogen, a sustainable energy source (Cammack *et al.*, 2001).

Three major classes of hydrogenases have evolved convergently (see Vignais & Billoud, 2007): the mono-iron hydrogenases ([Fe]-hydrogenases) or Hmds (H_2-forming methylenetetrahydromethanopterin dehydrogenases), the di-iron hydrogenases ([FeFe]-hydrogenases) and the [NiFe]-hydrogenases.

The catalytic centre of the [NiFe]-hydrogenases contains Fe and Ni atoms coordinated by the thiol groups of four conserved cysteines. Furthermore, in the vast majority of [NiFe]-hydrogenases known to date one CO and two cyanides are coordinated at the iron. The assembly of the [NiFe] active site and thus the integration of the diatomic ligands has predominantly been investigated using hydrogenase 3 from *Escherichia coli* (Blokesch & Böck, 2002). The products of a set of six *hyp* (*hy*drogenase *p*leiotropic) genes, *hypABCDEF*, are necessary for active-site incorporation, and, in some cases, an additional *hyp* gene (*hypX*; Buhrke & Friedrich, 1998; Schwartz *et al.*, 2003) is also required. Organism-specific duplications and modifications of gene products can also play a role in [NiFe]-hydrogenase maturation, leaving a number of questions unresolved (Wolf *et al.*, 1998). The proteins encoded by *hypA* and *hypB* are responsible for nickel allocation (Atanassova & Zamble, 2005; Maier *et al.*, 1995).

Incorporation of the iron and the diatomic ligands relies on the proteins encoded by *hypCDE* and *hypF*. HypC forms distinct complexes with the large subunit of the hydrogenase (Blokesch & Böck, 2002; Winter *et al.*, 2005) and the maturation proteins HypD and HypE (Jones *et al.*, 2004). This indicates a function for HypC as a bilateral chaperone that interacts with two partners: the catalytic subunit and HypD. The maturation protein HypD contains nine conserved cysteine residues. While four of these residues coordinate a [4Fe–4S] cluster, the others have been proposed to act as a thiol redox-signalling pathway for cyanation of the active-site iron (Blokesch & Böck, 2006; Watanabe *et al.*, 2007). An iron-binding site has been hypothesized within the HypCD complex.

While the source of CO remains unclear (Roseboom *et al.*, 2005), the cyanide ligands are derived from carbamoyl phosphate provided by HypE and HypF (Lenz *et al.*, 2007; Forzi *et al.*, 2007). The HypF protein first couples ATP hydrolysis to the synthesis of a carbamoyl-AMP complex and then transfers the carbamoyl moiety to the C-terminal cysteine residue in the conserved PR(V/I)C motif of HypE (Reissmann *et al.*, 2003; Watanabe *et al.*, 2007). The resulting HypE-thiocarboxamide is transformed into HypE-thiocyanate in a reaction coupled to ATP hydrolysis. The cyanide ligand is reductively transferred to HypCD (Blokesch & Böck, 2002).

On the basis of DNA-sequence analysis, *E. coli* HypF and homologous proteins accommodate three major functional domains: an N-terminal acylphosphatase domain, two zinc-finger motifs and a C-terminal *O*-carbamoyltransferase domain (Paschos *et al.*, 2002; Wolf *et al.*, 1998). Acylphosphatases usually catalyze ATP-independent cleavage of an acylphosphate into carboxylate and phosphate. Nonetheless, it has been shown that ATP can be a competitive inhibitor (Paoli *et al.*, 2000). Carbamoyltransferases transfer the carbamoyl group to an acceptor in an ATP-dependent fashion (Freel Meyers *et al.*, 2004).

While structures of HypCD and HypE from several organisms are now available (Watanabe *et al.*, 2007; Shomura *et al.*, 2007; Rangarajan *et al.*, 2008), only the N-terminal acylphosphatase domain of HypF has been characterized *via* crystallography (Rosano *et al.*, 2002). This particular fragment has been used as a model for amyloid-fibril formation in neurodegenerative diseases (Bucciantini *et al.*, 2004). However, the structures of a complete HypF protein, of the remaining domains or even of homologous proteins are not yet available.

In addition to the HypF protein as described above, a truncated version has also been characterized. In *Ralstonia eutropha* this variant has been designated HypF1 (GeneID 2656435). The corresponding gene only encodes the C-terminal *O*-carbamoyltransferase domain and therefore the protein lacks more than 50% of the comparable *E. coli*-type HypF, including the acylphosphatase domain. HypF1 consists of 394 amino-acid residues and has a molecular mass of 40.7 kDa. While the majority of [NiFe]-hydrogenase-containing organisms harbour the larger version of HypF, several others possess only the truncated protein. In addition, some bacteria such as *R. eutropha* harbour genes coding for both HypF variants.

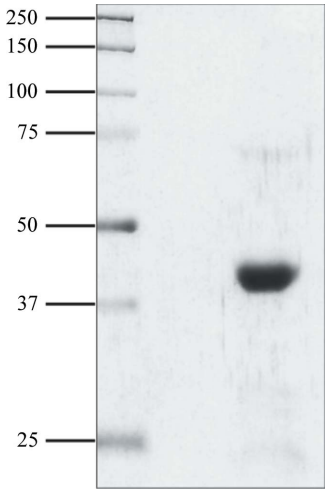

Figure 1
Silver staining of a 12% SDS–PAGE of the purified HypF1 protein (40.7 kDa). Protein Ladder (New England Biolabs) was used as a protein molecular-weight marker (molecular weights are labelled in kDa).

Mutational analysis has demonstrated that the truncated HypF1 in *R. eutropha* is sufficient for hydrogenase maturation (Wolf *et al.*, 1998). As the roles of this truncated protein in [NiFe]-hydrogenase maturation are unresolved, the crystal structure of HypF1 will shed light not only on the structure of full-length HypF but also on the distinct functions of the shorter HypF1 protein.

2. Material and methods

2.1. Expression and purification of HypF1

The construction of the vector pCH1053 used for the expression of HypF1 has been described previously (Jones *et al.*, 2004). The overexpression of the HypF1 protein harbouring a C-terminal Strep-Tag II (amino-acid sequence SAWSHPQFEK) was controlled using a modified version of the *R. eutropha acoX* promoter. The tagged version of the HypF1 protein consists of 404 amino-acid residues and has a slightly increased molecular mass of 41.8 kDa.

Cells were grown in mineral salts medium containing 0.4% fructose or a mixture of fructose and glycerol [0.2%(*w*/*v*) each; fructose–glycerol minimal medium (FGN); Schwartz *et al.*, 1998] using 10 l fermenters (Braun) for 48 h at 303 K to a final OD_{436} of 11. Expression of HypF1 was induced at an OD_{436} of 5 by the addition of acetoin to a final concentration of 1 m*M*. All purification steps were carried out at 277 K. The cells were harvested by centrifugation. The pellet was resuspended in 100 m*M* Tris–HCl buffer pH 8, 150 m*M* NaCl (Strep-Tag buffer *A*) and disrupted by three passages through a chilled French pressure cell (SLM-Aminco, Rochester, USA) at 7.58 MPa. Cell debris and membranes were separated from the soluble fraction by ultracentrifugation for 45 min at 90 000*g*. The soluble extract was loaded onto a glass column (Applied Biosystems) filled with 3 ml Strep-Tactin Superflow (IBA, Göttingen, Germany). The extract was applied in 5 ml fractions with 1 ml washes between each application on a BioCad Sprint Workstation (PE Biosystems) at 1.3 ml min^{-1}. Loosely bound proteins were removed by washing with ten column volumes (CV) of Strep-tag buffer *A* at 3.3 ml min^{-1}. Elution of the protein was performed at 1.3 ml min^{-1} using 15 CV 100 m*M* Tris–HCl pH 8, 150 m*M* NaCl, 5 m*M* desthiobiotin (Strep-tag buffer *B*). The column material was regenerated using 40 CV of 100 m*M* Tris–HCl pH 8, 150 m*M* NaCl, 5 m*M* HABA (Strep-tag buffer *C*) at 3.3 ml min^{-1}. Protein-containing fractions were pooled and concentrated in an Amicon Ultra-15 (Millipore) filtration device with a molecular-weight cutoff of 30 kDa. The buffer was also changed to 10 m*M* MOPS pH 7.5 by three additional centrifugation steps. The volume of the protein solution was reduced to less than 2 ml for size-exclusion chromatography. Using an ÄKTA Purifier 10 (Amersham Pharmacia), the protein solution was loaded onto a gel-filtration column (HiLoad 16/60 Superdex prep grade, Amersham Pharmacia) at 1 ml min^{-1} with 10 m*M* MOPS buffer pH 7.5 and 150 m*M* NaCl. Fractions containing pure protein were pooled, concentrated to a final concentration of approximately 10 mg ml^{-1} and buffer-exchanged to 10 m*M* MOPS pH 7.5 and 1.5 m*M* of the reducing agent TCEP–HCl (Hampton Research). The protein concentration was estimated by the method of Bradford (1976) and by the use of a microvolume spectrophotometer (ND-1000 Spectrophotometer, NanoDrop Technologies Inc.). The purity was verified by 12% SDS–PAGE (Fig. 1) and DLS measurements.

2.2. Crystallization

The hydrogenase maturation factor HypF1 was crystallized using the sitting-drop vapour-diffusion method. A broad variety of conditions were tested using kits from Hampton Research (Crystal Screen,

Crystal Screen 2, Crystal Screen Cryo, Low Ionic Strength Screen and Additive Screen) and Jena Bioscience (JBScreen Classic). Freshly purified protein at a concentration of 7 mg ml^{-1} was used immediately. The screening drops were prepared in CrystalQuick 96-well Greiner plates (Hampton Research) by mixing equal volumes (1–1.5 µl) of protein solution and crystallization solution. The plates were sealed with Clearseal Film (Hampton Research) and kept in a vibration-isolated box at a constant temperature of 293 K. After screening, crystals suitable for diffraction experiments were obtained by sitting-drop vapour diffusion using Linbro plates containing 24 wells each filled with 500 µl reservoir solution and Micro-Bridges (Hampton Research) with the following composition of the reservoir solution: 2.4 *M* sodium formate, 100 m*M* MOPS buffer pH 7.5, 100 m*M* $MgCl_2$. After mixing the protein and reservoir solutions Na_2ATP was added to the drop to give a final concentration of 0.5 m*M*. The crystals were grown at 285 K in a vibration-free crystallization refrigerator (Typ 3201, RUMED). Square-shaped crystal plates appeared after approximately 5 d with dimensions of 0.4 × 0.4 × 0.2 mm (Fig. 2).

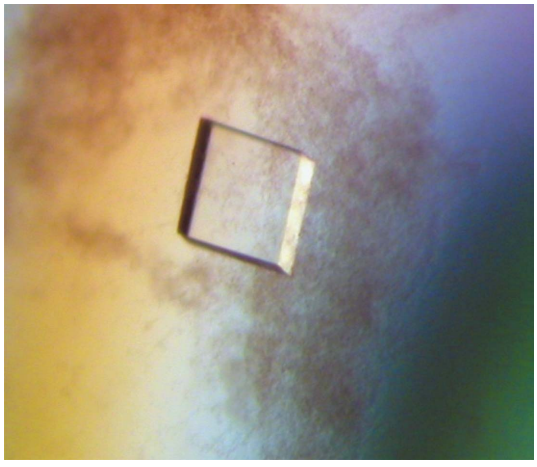

Figure 2
Crystal of the hydrogenase maturation protein HypF1 from *R. eutropha*. The crystal dimensions were 0.4 × 0.4 × 0.2 mm.

The methionine-auxotrophic strain HF41 (Friedrich *et al.*, 1981) of *R. eutropha* was tested for selenomethionine incorporation, but the material obtained was insufficient for crystallization experiments. Expression in *E. coli* strains was also ineffective. In order to obtain derivatives, crystals were transferred to drops of reservoir solution containing heavy-atom compounds. All screens tested (Platinum, Gold, Mercury, M1, M2; Hampton Research) were varied in concentration and soaking time. Crystals that were exposed for 12 h to 5 m*M* PIP [di-μ-iodobis(ethylenediamine)diplatinum(II) nitrate] remained stable and diffracting after back-soaking for 15 min in buffer lacking PIP. For cryoprotection, the crystals were transferred into drops of reservoir solution containing sodium formate at gradually increasing concentrations (2.4, 3.5 and 4.5 *M*) and flash-cooled in liquid nitrogen.

2.3. Data collection and processing

A large number of data sets of variable quality were collected from native crystals as well as from heavy-atom-soaked crystals. Only the best native and heavy-atom-derivative data sets collected so far are described here.

Diffraction data were collected at 100 K on beamlines 14.1 or 14.2 at BESSY of the Protein Structure Factory and Freie Universität Berlin (Berlin, Germany). The detector was a fast-scanning MX-225 CCD detector from Rayonics (Evanston, USA) mounted on a MARdtb goniostat from MAR Research (Norderstedt, Germany). For the native data, a set of 360 images of 10 s exposure time and 0.5° oscillation increments was collected (Fig. 3.).

The first evidence that platinum was incorporated in the putative PIP-derivative crystal after back-soaking was provided by the appearance of a clear platinum absorption edge as deduced from the X-ray fluorescence scan, enabling us to determine the peak (λ = 1.07225 Å) and inflection (λ = 1.07252 Å) wavelengths.

For the PIP derivative, separate sets of 360 images with 0.5° oscillation increments were measured at the peak and inflection wavelengths, but the lower quality of the inflection-wavelength data

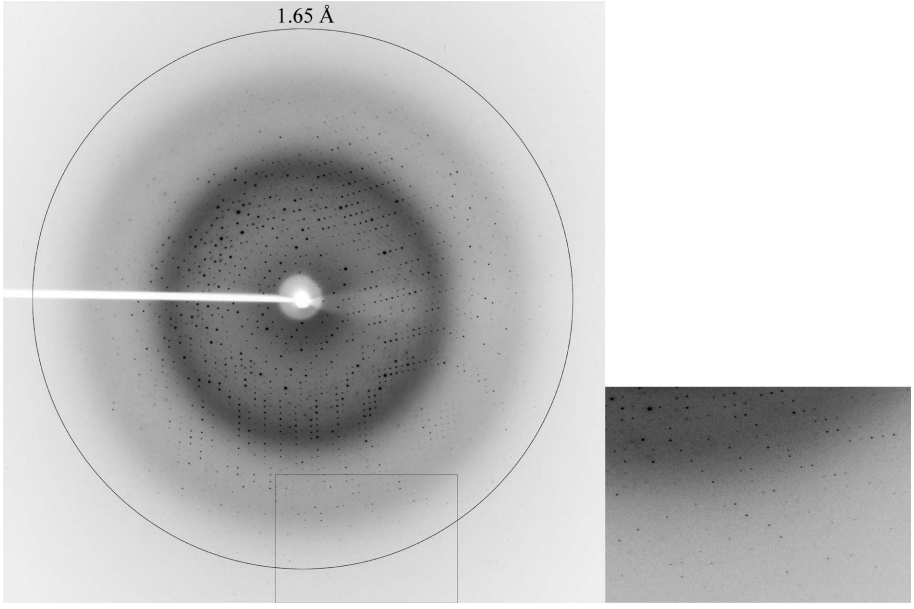

Figure 3
Diffraction image of a native HypF1 crystal with an enlarged view (right) of the area delimited by the rectangle. The circle marks a resolution of 1.65 Å.

Table 1
Data-collection statistics.

Values in parentheses are for the highest resolution shell.

		PIP derivative	
	Native	Peak	Inflection
Unit-cell parameters (Å)	a = 79.66, b = 91.64, c = 107.15	a = 80.22, b = 91.39, c = 106.00	
Space group	$I222$		
Wavelength (Å)	0.91841	1.07225	1.07252
Resolution (Å)	19.5–1.65 (1.75–1.65)	37.2–2.95 (3.12–2.95)	37.3–3.25 (3.44–3.25)
No. of measurements	173724	60709	45090
No. of unique reflections	46974	15798	11853
Completeness (%)	98.5 (98.1)	99.1 (95.0)	98.6 (91.7)
Redundancy	3.6 (3.7)	3.8 (3.8)	3.8 (3.5)
$\langle I/\sigma(I)\rangle$	15.9 (3.0)	11.3 (3.3)	12.8 (2.9)
$R_{\rm merge}$† (%)	4.5 (43.0)	9.4 (46.1)	8.1 (47.4)
Beamline	BESSY BL14.2	BESSY BL14.1	
No. of molecules in ASU	1		

† $R_{\rm merge} = \sum_{hkl}\sum_i |I_i(hkl) - \langle I(hkl)\rangle| / \sum_{hkl}\sum_i I_i(hkl)$, where $I_i(hkl)$ is the observed intensity of reflection hkl and $\langle I(hkl)\rangle$ is the averaged intensity of symmetry-equivalent measurements.

set indicated that the crystal had suffered from significant radiation damage, probably making it unsuitable for MAD phasing. However, analysis using *SHELXC* (Sheldrick, 2008) provided further evidence that derivatization using PIP was successful, since the correlation coefficient between the signed anomalous differences in the two data sets was still 31% in the resolution range 3.5–3.3 Å.

Data were indexed, integrated, scaled and merged using *XDS* (Kabsch, 1993). Further processing was performed using the *CCP*4 program suite (Collaborative Computational Project, Number 4, 1994).

3. Results and discussion

The [NiFe]-hydrogenase maturation protein HypF1 was purified with high quality from *R. eutropha* H16. The best crystallization results were obtained using the sitting-drop vapour-diffusion technique. The native crystals diffracted to 1.65 Å resolution and heavy-atom sites were identified for a platinum derivative. The crystals belonged to space group $I222$, with unit-cell parameters a = 79.7, b = 91.6, c = 107.2 Å. Assuming that the crystals contained one monomer per asymmetric unit, the solvent content was calculated to be 49%, with a crystal volume per protein mass $V_{\rm M}$ of 2.4 Å^3 Da^{-1} (Matthews, 1968).

Analysis revealed characteristics of the diffraction pattern that make structure solution a nontrivial challenge. Several data sets showed anisotropy and high mosaicity effects. Furthermore, a number of crystals showed reflections in addition to those consistent with the $I222$ unit cell. These reflections suggest either the breakdown of translational symmetry (body centring; orthorhombic P instead of orthorhombic I) in the crystals or the presence of a superlattice with the a axis being three times longer than in the original unit cell or both, depending on the individual crystal. The intensity statistics of these data sets indicated twinning or pseudo-translational symmetry. Attempts to explain the observed features in the diffraction patterns by nonmerohedral twinning assuming that the true unit cell is that given in Table 1 failed. Even those crystals, including those for which the diffraction data are summarized in Table 1, which appeared to be true single crystals without any superlattice/pseudo-translation features turned out to be non-isomorphous to each other after scaling, thus preventing the determination of phases by combination of the corresponding data sets.

This study reports the successful crystallization of the maturation protein HypF1 from *R. eutropha* H16. As no homologous structure is available to date, the structure could not be solved by molecular replacement. Efforts to resolve the irregularities in the diffraction patterns are in progress.

This work was supported by the Deutsche Forschungsgemeinschaft, SFB 498-C1 'Bacterial [NiFe]-hydrogenases: key reactions of the biological activation of molecular hydrogen' (to BF, WH und NK). AKJ acknowledges the Humboldt Foundation for a fellowship. The authors thank Uwe Müller and the scientific and technical staff of BESSY-MX at BESSY II (Berlin, Germany) as well as Victor Lamzin, Manfred Weiss and the scientific and technical staff of the EMBL Outstation at DESY (Hamburg, Germany) for continuous support of this project. We are also grateful to Helga Wessner for assistance and crystallization advice.

References

Atanassova, A. & Zamble, D. B. (2005). *J. Bacteriol.* **187**, 4689–4697.
Blokesch, M. & Böck, A. (2002). *J. Mol. Biol.* **324**, 287–296.
Blokesch, M. & Böck, A. (2006). *FEBS Lett.* **580**, 4065–4068.
Bradford, M. M. (1976). *Anal. Biochem.* **72**, 248–254.
Bucciantini, M., Calloni, G., Chiti, F., Formigli, L., Nosi, D., Dobson, C. M. & Stefani, M. (2004). *J. Biol. Chem.* **279**, 31374–31382.
Buhrke, T. & Friedrich, B. (1998). *Arch. Microbiol.* **170**, 460–463.
Cammack, R., Frey, M. & Robson, R. (2001). *Hydrogen as a Fuel.* London: Taylor & Francis.
Collaborative Computational Project, Number 4 (1994). *Acta Cryst.* D**50**, 760–763.
Forzi, L., Hellwig, P., Thauer, R. K. & Sawers, R. G. (2007). *FEBS Lett.* **581**, 3317–3321.
Freel Meyers, C. L., Oberthür, M., Xu, H., Heide, L., Kahne, D. & Walsh, C. T. (2004). *Angew. Chem. Int. Ed.* **43**, 67–70.
Friedrich, B., Hogrefe, C. & Schlegel, H. G. (1981). *J. Bacteriol.* **147**, 198–205.
Jones, A. K., Lenz, O., Strack, A., Buhrke, T. & Friedrich, B. (2004). *Biochemistry*, **43**, 13467–13477.
Kabsch, W. (1993). *J. Appl. Cryst.* **26**, 795–800.
Lenz, O., Zebger, I., Hamann, J., Hildebrandt, P. & Friedrich, B. (2007). *FEBS Lett.* **581**, 3322–3326.
Maier, T., Lottspeich, F. & Böck, A. (1995). *Eur. J. Biochem.* **230**, 133–138.
Matthews, B. W. (1968). *J. Mol. Biol.* **33**, 491–497.
Paoli, P., Camici, G., Manao, G., Giannoni, E. & Ramponi, G. (2000). *Biochem. J.* **349**, 43–49.
Paschos, A., Bauer, A., Zimmermann, A., Zehelein, E. & Böck, A. (2002). *J. Biol. Chem.* **277**, 49945–49951.
Rangarajan, E. S., Asinas, A., Proteau, A., Munger, C., Baardsnes, J., Iannuzzi, P., Matte, A. & Cygler, M. (2008). *J. Bacteriol.* **190**, 1447–1458.
Reissmann, S., Hochleitner, E., Wang, H., Paschos, A., Lottspeich, F., Glass, R. S. & Böck, A. (2003). *Science*, **299**, 1067–1070.
Rosano, C., Zuccotti, S., Bucciantini, M., Stefani, M., Ramponi, G. & Bolognesi, M. (2002). *J. Mol. Biol.* **321**, 785–796.
Roseboom, W., Blokesch, M., Böck, A. & Albracht, S. P. J. (2005). *FEBS Lett.* **579**, 469–472.
Schwartz, E., Gerischer, U. & Friedrich, B. (1998). *J. Bacteriol.* **180**, 3197–3204.
Schwartz, E., Henne, A., Cramm, R., Eitinger, T., Friedrich, B. & Gottschalk, G. (2003). *J. Mol. Biol.* **332**, 369–383.
Sheldrick, G. M. (2008). *Acta Cryst.* A**64**, 112–122.
Shomura, Y., Komori, H., Miyabe, N., Tomiyama, M., Shibata, N. & Higuchi, Y. (2007). *J. Mol. Biol.* **372**, 1045–1054.
Vignais, P. M. & Billoud, B. (2007). *Chem. Rev.* **107**, 4206–4272.
Watanabe, S., Matsumi, R., Arai, T., Atomi, H., Imanaka, T. & Miki, K. (2007). *Mol. Cell*, **27**, 29–40.
Winter, G., Buhrke, T., Lenz, O., Jones, A. K., Forgber, M. & Friedrich, B. (2005). *FEBS Lett.* **579**, 4292–4296.
Wolf, I., Buhrke, T., Dernedde, J., Pohlmann, A. & Friedrich, B. (1998). *Arch. Microbiol.* **170**, 451–459.